JOURNAL OF GEOPHYSICAL RESEARCH, VOL. 105, NO. A8, PAGES 18,169–18,185, AUGUST 1, 2000

Properties of coronal mass ejections: SOHO LASCO observations from January 1996 to June 1998

O. C. St. Cyr,[1] R. A. Howard,[2] N. R. Sheeley Jr.,[2] S. P. Plunkett,[3] D. J. Michels,[3] S. E. Paswaters,[4] M. J. Koomen,[5] G. M. Simnett,[6] B. J. Thompson,[7] J. B. Gurman,[7] R. Schwenn,[8] D. F. Webb,[9,10] E. Hildner,[11] and P. L. Lamy[12]

Abstract. We report the properties of all the 841 coronal mass ejections (CMEs) observed by the Solar and Heliospheric Observatory (SOHO) Large Angle Spectroscopic Coronagraph (LASCO) C2 and C3 white-light coronagraphs from January 1996 through June 1998, and we compare those properties to previous observations by other similar instruments. Both the CME rate and the distribution of apparent locations of CMEs varied during this period as expected based on previous solar cycles. The distribution of apparent speeds and the fraction of CMEs showing acceleration were also in agreement with earlier reports. The pointing stability provided by an L-1 orbit and the use of CCD detectors have resulted in superior brightness sensitivity for LASCO over earlier coronagraphs; however, we have not detected a significant population of fainter (i.e., low mass) CMEs. The general shape of the distribution of apparent sizes for LASCO CMEs is similar to those of earlier reports, but the average (median) apparent size of 72° (50°) is significantly larger. The larger average apparent size is predominantly the result of the detection of a population of partial and complete halo CMEs, at least some of which appear to be events with a significant longitudinal component directed along the Sun-Earth line, either toward or away from the Earth. Using full disk solar images obtained by the Extreme ultraviolet Imaging Telescope (EIT) on SOHO, we found that 40 out of 92 of these events might have been directed toward the Earth, and we compared the timing of those with the *Kp* geomagnetic storm index in the days following the CME. Although the "false alarm" rate was high, we found that 15 out of 21 (71%) of the $Kp \geq 6$ storms could be accounted for as SOHO LASCO/EIT frontside halo CMEs. If we eliminate three *Kp* storms that occurred following LASCO/EIT data gaps, then the possible association rate was 15 out of 18 (83%).

1. Introduction

The dynamic processes taking place in the rarified atmosphere of our nearest star are sufficient motivation for many researchers to examine the Sun, the heliosphere, and planetary magnetospheres as plasma physics laboratories. But recent research connecting severe geomagnetic disturbances directly with coronal mass ejections from the Sun [e.g., *Gosling*, 1993] has renewed interest in a more systemic approach to the arcane specialties of solar and space physics (e.g., collection of reports by *Russell* [1995]). The observations described here were obtained as part of an international effort (known within NASA as the International Solar Terrestrial Physics program) to bridge the gaps between scientific specialties and to continue to build the foundation for a physics-based, applied science in the future.

This manuscript describes recent observations of coronal mass ejections near the Sun. These sporadic ejections of material through the Sun's atmosphere into interplanetary space can be detected remotely (both by imaging and by inference) at many wavelengths across the electromagnetic spectrum (e.g., X ray, EUV, Hα, and radio). Also the plasma, particle, and magnetic properties of ejected material can be measured in situ in the heliosphere. However, the phrase "coronal mass ejection" was initially coined to describe the detection of new, discrete, bright features appearing in the field of view of a white-light coronagraph and moving outward over a period of minutes to hours [e.g., *Munro et al*., 1979]. On the basis of that definition we report here the statistical characteristics of coronal mass ejections (CMEs) detected by the externally occulted coronagraphs onboard the European Space Agency (ESA)/NASA Solar and Heliospheric Observatory (SOHO) spacecraft [*Domingo et al*., 1995].

The understanding of the origin, observation, and effects of CMEs has benefited from significant effort during the past 25 years, and the reader is directed to any of the recent reviews describing our current knowledge and lack thereof [e.g., *Sch-*

[1]Computational Physics, Inc., Fairfax, Virginia.
[2]Naval Research Laboratory, Washington, D. C.
[3]Universities Space Research Association, Washington, D. C.
[4]Ball Aerospace Corporation, Boulder, Colorado.
[5]Sachs Freeman Associates, Largo, Maryland.
[6]School of Physics and Space Research, University of Birmingham, Birmingham, United Kingdom.
[7]NASA Goddard Space Flight Center, Greenbelt, Maryland.
[8]Max Planck Institut fur Aeronomie, Lindau, Germany.
[9]Institute for Scientific Research, Boston College, Chestnut Hill, Massachusetts.
[10]Also at Air Force Research Laboratory, Space Vehicles Directorate, Hanscom AFB, Massachusetts.
[11]NOAA Space Environment Center, Boulder, Colorado.
[12]Laboratoire d'Astronomie Spatiale, Marseille, France.

Paper number 1999JA000381.
0148-0227/00/1999JA000381$09.00

wenn, 1995; *Hundhausen*, 1999; *Gosling*, 1999]. The format of the initial part of this manuscript will be similar to other statistical surveys of large numbers of CMEs so that relevant comparisons can be drawn. However, there are new aspects to these data that exceed results from previous coronagraphs and that extend the SOHO results to the prediction of near-Earth space environmental conditions.

The CME observations reported here were obtained by the Large Angle Spectroscopic Coronagraph (LASCO) onboard SOHO [*Brueckner et al*., 1995]. LASCO consists of a suite of three coronagraphs, but the results described here were obtained with the two externally occulted telescopes (C2 and C3). The third component of the LASCO suite (C1, an internally occulted, reflective instrument observing the emission line corona) also detected some CMEs [e.g., *Plunkett et al*., 1997; *Schwenn et al*., 1997], but data from it have not been considered in this survey so that the aforementioned comparison with earlier broadband white-light CME observations can be made directly.

Examples of individual or small numbers of SOHO LASCO CME observations exist in the literature [e.g., *Dere et al*., 1997; *Chen et al*., 1997; *Simnett et al*., 1997]. Statistics of CMEs based on a three month period in 1997 were reported by *St. Cyr et al*. [1997]; but this is the first study to provide a statistical view of the properties of coronal mass ejections observed by LASCO during the 2.5 year nominal mission life.

2. Description of Observations

The observations described here cover the nominal mission phase of SOHO, from January 1996 through June 24, 1998. The LASCO instrument commissioning activities began after the December 2, 1995, launch; the first LASCO C3 observations considered in this CME statistical study were obtained on January 9, 1996, and continued sporadically until the insertion of SOHO into a halo orbit about the Lagrangian L-1 point. Instrument check-out activities were completed by late April 1996; and a synoptic cadence of images from C2 and C3 commenced in early May 1996. There were intermittent interruptions to that cadence due to spacecraft and instrument anomalies and activities, but an adequate duty cycle to detect and to characterize CMEs (described below) was maintained until the unintentional loss of contact with the spacecraft in late June 1998. Operations with SOHO resumed in October 1998 and continue at the time of this writing; however, these more recent observations will be described in future work.

Most of the LASCO C2 (C3) data surveyed were images acquired through the broad bandpass Orange (Clear) filter. The nominal field of view for C2 (C3) includes solar heights from 2.0 to 7.0 (3.7–32.0) R_{Sun}, as measured in a heliocentric coordinate system where 1.0 R_{sun} is equivalent to the limb of the visible disk of the Sun. Nominal exposure durations were 25s (19s) for C2 (C3), and onboard compression of the CCD-detected image was typically done with a lossless or a slightly lossy (typically a factor of less than 8 times compression for C2 and 7 times compression for C3) algorithm.

Normally, a single image was obtained from each telescope about once per hour; a single set of polarization and color sequences were also acquired from each telescope during a typical 24 hour schedule. Prior to February 1997 the north and south polar regions of the C2 and C3 image frames were often truncated into an "equatorial" field to conserve onboard computing and telemetry resources. The acquisition of additional telemetry after February 1997 provided resources for more frequent C2 images and allowed acquisition of full-frame images rather than equatorial versions for both telescopes.

As with any solar instrument observing from an L-1 platform, the coronagraphs have benefited in several ways by the elimination of the ~15 day/night transitions per 24 hours that are typical for a satellite in low-Earth orbit. Foremost is the elimination of the cyclic interruptions in observations that complicate the detection and tracking of CMEs. More importantly, at L-1 the thermal shock and resulting mechanical deformation that arise from the day/night transitions are eliminated. This not only provides a more favorable thermal environment for the optical bench supporting any given coronagraph, an instrument that has stringent pointing stability requirements, but it eliminates the need to recenter the telescope after each orbital sunrise. Both factors contribute to a stable, instrumental stray light level that can be calibrated and removed to detect faint coronal features.

3. Identification of CMEs

All of the relevant C2 and C3 images from January 1996 through June 1998 have been examined for the presence of coronal mass ejections. This examination was carried out by an observer viewing a computer monitor, toggling through sequential image frames from each coronagraph. This process included routine examination of both direct images (with only a background subtracted) and difference images, whereby each image was digitally subtracted pixel-by-pixel from an earlier frame, allowing the detection of faint new enhancements in the field of view. In fact, these are the same techniques used previously for detection of CMEs in the data from the Solwind instrument on U.S. Air Force satellite P78-1 [*Howard et al*., 1985], from NASA's Solar Maximum Mission (SMM) coronagraph [*Burkepile and St. Cyr*, 1993], and from the Mauna Loa Solar Observatory (MLSO) MK3 k-coronameter [*St. Cyr et al*., 1999]. Thus comparison of LASCO statistics with these earlier data sets should be valid, since the techniques and the observers are the same. (Note the film images from the Skylab instrument [*MacQueen et al*., 1976] have recently been digitized, but reduction of those data using modern image processing techniques to identify CMEs has not yet been performed.)

The LASCO CME compilation for this period was produced predominantly by one of us (OCS) and made available online (http://lasco-www.nrl.navy.mil/cmelist.html) for the use of researchers with complementary observations. This compilation has been checked by iteration and by comparison with other listings maintained within the LASCO team. However, our experience from Solwind, SMM, and MLSO suggests that any CME compilation must be viewed as a living document, which may change as new image processing methods and new ideas and biases are applied. The statistical description and results of this manuscript are based on the CME compilation as of this writing.

The Skylab researchers classified all significant coronal changes as "transients," but they identified mass ejections as being that subset where there was clear evidence of outward motion. Similarly, a classification called "coronal anomaly" was identified in Solwind, SMM, and MLSO when changes were detected but outward motion could not be identified unambiguously. We can illustrate the magnitude of this with examples: the SMM anomaly listing was about half the size of the CME listing (628 anomalies versus 1351 CMEs); for MLSO an even

Table 1. Detector Comparison for Dynamic Range Definition

	Solwind SEC Vidicon	SMM SEC Vidicon	SOHO LASCO CCD
Typical noise level	~2 DN	~5 DN	~1–2 DN
Typical background level	~20 DN	~10 DN	~1,000 DN for C2 at ~6.0 R_{sun} for C3 at ~30.0 R_{sun}
Typical coronal brightness level	~60 DN	~160 DN	~8,000 DN for C2 streamer at ~2.5 R_{sun} for C3 streamer at ~6.0 R_{sun}
Typical saturation level	~65–127 DN	~200–240 DN	~12,000 DN for C2 at ~1.8 R_{sun} for C3 at ~3.5 R_{sun}
Resulting dynamic range	~30	~40	~6,000

Comparison of typical detector digitization values (DN = digital number) for the Solwind, SMM, and LASCO coronagraphs. The LASCO CCD quantization step was set to ~15 electrons. Since full-well capacity is ~150,000 electrons, then a dynamic range of 10,000 is theoretically possible. For LASCO C2 and C3, the exposure times are set so that the brightest portion of the image (the brightest diffraction rings surrounding the occulter shadow) is just at or below saturation level.

larger fraction of transients were classified as "anomaly" (195 anomalies versus 246 CMEs). However, in a detailed event-by-event comparison, *St. Cyr et al*. [1999] found that only 5% of the MLSO CMEs had been classified as "anomaly" in SMM.

With LASCO C2 and C3 we have the advantage of two separate coronagraphs, operating continuously, with near simultaneity and with overlapping fields of view. It is difficult to quantify the improvement gained in identifying extremely faint transients as "anomaly" versus "CME," but we estimate that ~5% of the total number of CMEs in our compilation may have been "upgraded" from anomaly to CME based on the appearance of the event in both coronagraphs. At least two additional classes of coronal transients, both discovered in LASCO data, have been intentionally excluded from this compilation: (1) the polar microjets reported by *Moses et al*. [1997] and by *Wang et al*. [1998] and (2) the small inhomogeneities that may trace out the low latitude acceleration of the slow solar wind [*Sheeley et al*., 1997]. Both types of transients have been detected as frequently as a few times per day, but their appearance is highly sporadic. A few similar events may have been recognized and included in Solwind and SMM catalogs of CMEs. Although both classes of transients appear to satisfy the definition of "new bright material appearing in the corona on timescales of minutes to hours and moving outward," their status in the hierarchy of coronal disturbances does not currently seem to warrant inclusion as CMEs. Future researchers may wish to revise the definition as new information is gathered, but we have limited inclusion to this compilation to ejections that have an apparent angular size of at least 5°.

The CME compilation identifies the time (in UT) that new bright material was first detected in C2. For some events a CME was "in progress" in the field of view when observations resumed following a data gap (13 instances), some CMEs were first detected in C3 (12 cases), and some CMEs were both "in progress" and first detected in C3 (8 instances). Most of the CMEs with these qualifiers were detected in early 1996, during the instrument commissioning activities. Those few events detected only in C3 occurred when C2 observations were not available.

The CCD detectors used by LASCO have a much larger dynamic range than previous spaceborne coronagraphs. Detailed descriptions of those cameras were given by *Brueckner et al*. [1995], but it is worthwhile to examine the LASCO brightness sensitivity in the context of the CME observations described here. Since the phrase "dynamic range" appears to have several accepted definitions, we have tabulated relevant detector values that we consider typical in Table 1. We have defined dynamic range as the ratio of the digital value where pixels become saturated to the digital value of the lowest measurable signal (i.e., noise level). The contrast of a CME is frequently described in terms of a $(\Delta B/B_{\text{background}})$ ratio, defined as the maximum change in coronal brightness (ΔB) compared to the background corona $(B_{\text{background}})$. *Sime and Hundhausen* [1987] noted that the $(\Delta B/B_{\text{background}})$ ratio ranged from a few percent for the faintest CMEs up to unity for the brightest events. Of course, in any imaging detector, there are pixel-to-pixel and even area-wide variations, and often the corners and edges of the field of view are less sensitive. However, the improvement in sensitivity of the LASCO CCD detectors over the Solwind and SMM vidicon detectors is remarkable.

The spatial resolution of C2 was similar to SMM. If we assume that instrumental factors (e.g., vignetting and stray light) were similar, the LASCO CCD therefore affords the possibility of detecting much fainter mass ejections than earlier instrumentation. Previous reports based on CME mass distributions from Solwind [*Jackson and Howard*, 1993] and Helios [*Jackson and Webb*, 1994] indicated a decrease in the fraction of "small" (fainter, hence less massive) events, but those studies could not rule out the possibility of instrumental limitations. Intensity calibration and threshold determination for C2/C3 are incomplete as of this writing, but we can report that the LASCO data appear to support the conclusion of the earlier work; despite the enormous increase in dynamic range, we have not detected a significantly enhanced population of fainter CMEs beyond those expected due to plane of the sky projections.

A rigorous examination of the LASCO visibility function will be performed in the future when sufficient numbers of metric Type II radio bursts have been detected to undertake such a statistical analysis. The visibility function was the method employed for the Skylab, Solwind, and SMM coronagraph observations to account for the decreased sensitivity of those instruments in detecting mass ejections out of the plane of the sky

Table 2. Annual and Cumulative SOHO LASCO CME Statistics

Dates	Number of CMEs	CME Rate (uncertainties), CMEs/day	Average (rms) Apparent Latitude	Average (Median) Apparent Size	Average (Median) Apparent Speed	Number of Halo (360°) CMEs
Jan. 1 to Dec. 31, 1996	171	0.63 (−0.16)(+0.88)	−5° (24°)	54° (39°)	339 km/s (297 km/s)	3
Jan. 1 to Dec. 31, 1997	276	0.80 (−0.04)(+0.20)	+1° (23°)	82° (57°)	378 km/s (330 km/s)	17
Jan. 1 to Dec. 31, 1998	394	2.33 (−0.08)(+0.15)	+3° (35°)	72° (52°)	472 km/s (401 km/s)	16
Total	841		+1° (29°)	72° (50°)	424 km/s (360 km/s)	36

Annual statistical properties of coronal mass ejections observed by SOHO LASCO C2/C3.

[*Webb and Howard*, 1994]. The association of CMEs with metric Type II bursts is not one-to-one. Although the appearance of a CME is believed by many researchers (including *Webb and Howard* [1994]) to be a necessary condition for the detection of a metric Type II, it is not a sufficient condition as will be demonstrated in the following example from the SOHO era.

We have performed a preliminary analysis of all 80 metric Type II radio bursts reported during this period. We found that 67 bursts apparently were associated with the appearance of LASCO CMEs, assuming reasonable timing (e.g., CME appearance in LASCO within ±30 min of the reported start of the metric Type II) and reasonable spatial coincidence (when it was known from Hα flare reports for the Type II). Another nine Type II's appeared while a LASCO CME was in progress, so it was difficult to tell if new material appearing in the coronagraph field was part of the event in progress or if it was a new CME. Thus 76/80 (95%) of the metric Type II bursts in this preliminary survey were considered associated with LASCO CMEs [*Cliver et al*., 1998]. This indicates that little, if any, correction will be required as a visibility function for detection of CMEs for LASCO.

There were 841 coronal mass ejections identified in the LASCO C2/C3 data set between January 9, 1996, and June 24, 1998. Tabulated annual values are presented in Table 2, along with statistical measures described in detail in sections 4, 5, and 6. *Subramanian et al*. [1999] reported a significantly lower number of CMEs detected in these same data (375 versus 841 or 44%), but we believe that the statistics reported here should be valid for comparisons with previous studies.

4. CME Rate

The CME rate for LASCO C2/C3 is displayed in Figure 1, where values have been calculated for each 27.3 day Carrington Rotation of the Sun. The horizontal error bars represent the width of a Carrington Rotation, which we take as a measure of the inherent uncertainty in our knowledge of the true heliographic longitude of a CME, based on white light coronagraph data alone. The CMEs were assigned to individual rotations based on the Carrington Longitude of the Sun's central meridian at the time of the first appearance of the event, as described above. This method would certainly be incorrect if one were attempting to associate other forms of activity with the appearance of each CME, since one cannot determine the true location (or longitudinal extent) of a coronal mass ejection based on white-light coronagraph observa-

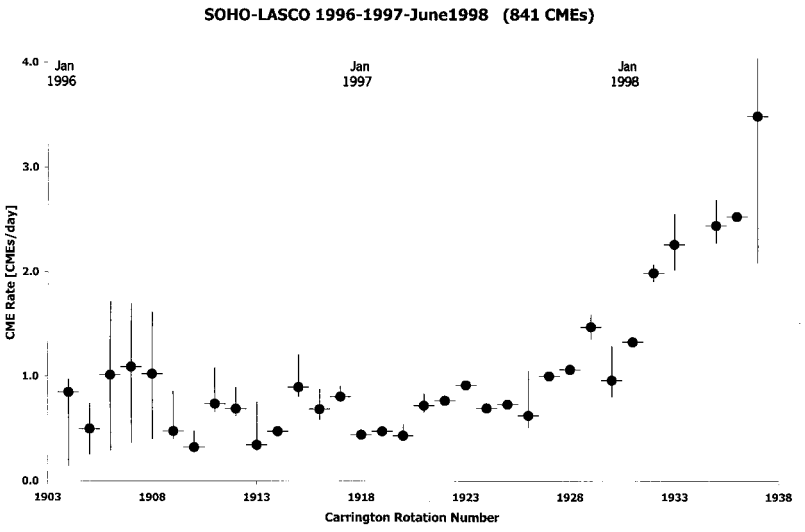

Figure 1. CME Rate plot versus Carrington Rotation. Uncertainties in the rate are duty cycle dependent, as explained in the text. Horizontal bars represent the inherent uncertainty of coronagraphic observations in determining the Carrington longitude and rotation of any given CME.

tions alone. The nature of Thomson scattering of photospheric light by electrons relegates optically thin structures such as CMEs to appear projected onto the plane of the sky. Without additional knowledge of the location of the structure (as from an EUV image of the low corona), we know the heliographic longitude of the event only within a factor of $\pm 90°$ from the plane of the sky. While this method would not be employed to examine the CME rate over only a few solar rotations, we believe that it is adequate (and instructive) to illustrate the rate over a duration of several years. The vertical uncertainties shown in Figure 1 are derived from a calculation of the observational duty cycle for LASCO to detect coronal mass ejections. An exhaustive treatise on this topic is given by *Hundhausen et al*. [1984], and we follow the basic method outlined there whereby the duty cycle is based on the average speed of a population of CMEs through the coronagraph field of view. The duty cycle for LASCO was based on C3 coverage alone; we consider this acceptable because C2 and C3 operated in tandem during almost the complete period considered in this survey. A "data gap" was declared if sequential C3 images were more than 180 min (3 hours) apart. A CME traveling 400 km/s (a reasonable value for the average speed of a population of white light CMEs) would cross the C3 field of view in 10.6 hours; so images taken more frequently than that should result in the direct detection of each event. However, other factors must be considered in determining the definition of data gaps, including the fact that the brightness of many CMEs is significantly reduced in the outer portion of the C3 field of view. (This point will be addressed in section 6.) Further, during 1996, some C2 and C3 frames were truncated into an "equatorial" field of view to conserve onboard computing and telemetry resources. This truncated field extended along the north-south direction in C2 (C3) to 3.6 R_{Sun} (15 R_{Sun}). As we will demonstrate below in section 5, mass ejections during this phase of the solar activity cycle appeared predominantly at or near the solar equator, so this restricted field did not negatively impact the statistical assessment described here. Hence we believe the 3 hour data gap threshold to be realistically (if not overly) conservative.

Data gaps were tallied by Carrington Rotation, and the CME rate for each solar rotation was determined as the ratio of the number of CMEs detected during that rotation, divided by the equivalent number of days observed during that rotation. The lower limit shown by the vertical error bars in Figure 1 is the CME Rate assuming no additional CMEs occurred during any data gaps in that rotation. The upper limit of the vertical uncertainties assumes that the maximum number of CMEs (defined as the maximum number occurring during any given 24 hour period during that rotation) were missed during each 24 hour data gap. A similar quantification of the CME rate was reported for Solwind and SMM by *Cliver et al*. [1994].

Note that the vertical error bars in Figure 1 for the first few rotations are larger than for subsequent rotations. As mentioned before, during the initial months of operation, both spacecraft and instrument commissioning and calibration activities prevented a routine synoptic cadence. Similarly, the vertical uncertainties during the final rotation in June 1998 are large because only a portion of that rotation was observed before the interruption in observations. We can compare Figure 1 and Table 2 to the annualized CME rates reported by *Webb and Howard* [1994]. As mentioned in section 3, those authors used Skylab, Helios, Solwind, and SMM observations of CMEs to determine an annual rate, and they corrected the observed values for both duty cycle and visibility function. The latter was determined from an analysis of metric Type II radio bursts, and it amounted to a corrective factor of 1.3 (Solwind) and 1.4 (Skylab and SMM) to the rates already corrected for duty cycle. Their reported values for years which would be considered solar activity minimum phase (1984, 1985, and 1986) ranged from 0.31 to 0.77 CMEs/day; and the rate for years of solar activity maximum (1979, 1980, and 1989) ranged from 1.75 to 3.11 CMEs/day.

Certainly much of the 1996 to early 1997 period would be considered solar activity minimum conditions, based on any of the common indicators [e.g., *Harvey and White*, 1999]. The steady rise of solar activity toward maximum levels (at least as measured by CME rate) is evident in Figure 1 during late 1997 into mid-1998. On the basis of the discussion in section 3, we believe that any visibility function correction to the CME rate derived from LASCO will be small or nonexistent. Hence we believe Figure 1 and Table 2 demonstrate that the 2.5 year era of LASCO observations is in reasonable agreement with both the phase and the magnitude of the *Webb and Howard* [1994] report. This is perhaps surprising since there is no reason to expect the CME rate to vary in the same fashion from one solar cycle to the next, but these data appear to show comparable rates to the two previous solar cycles. Moreover, this result indicates that the population of CMEs out of the sky plane and not detected by Solwind and SMM was properly accounted for by the visibility function used by *Webb and Howard* [1994].

5. Apparent Locations and Sizes of CMEs

The measurements of the apparent location and apparent size of a CME are linked, in that the apparent central position angle (measured counterclockwise from the projection of the Sun's north pole) is the bisector of the apparent span of the mass ejection. That measurement was possible for all but one (840/841) of the CMEs detected by LASCO, and, where data were available, it was performed in C2 as close to the occulting disk as possible (typically 2.0–2.5 R_{Sun}).

We have converted the apparent central position angle measurements to apparent latitudes as a more meaningful parameter. The distribution of apparent central latitudes is shown on an annual basis in Figure 2, with the cumulative distribution shown in Figure 2d. The distribution of apparent locations is more-or-less symmetric about and peaked near the solar equator (the average latitude is $+1°$). This is particularly true during 1996–1997, where over 50% of the events have central latitudes within $\pm 10°$ of the equator. This clustering is characteristic of the phase of the solar activity cycle we would consider solar minimum. The flattening of the equatorial peak to include higher latitudes in the cumulative distribution is predominantly a result of the CMEs detected during 1998, which accounted for 47% of the total. The category "halo" CMEs are those events that extend completely around the occulting disk (i.e., they have an apparent width of 360°), so they do not have an assigned apparent latitude. We suggest that the small number of these events (e.g., 1996 had three events with 360° span) makes it questionable to compare absolute numbers or even frequency between any given years, at least within this data set. These and other mass ejections with large apparent angular widths will be discussed in section 7.

On the basis of the earlier observations of Skylab, Solwind, and SMM, the CME span was characterized as the bright portion of the transient, and obvious deflections of preexisting

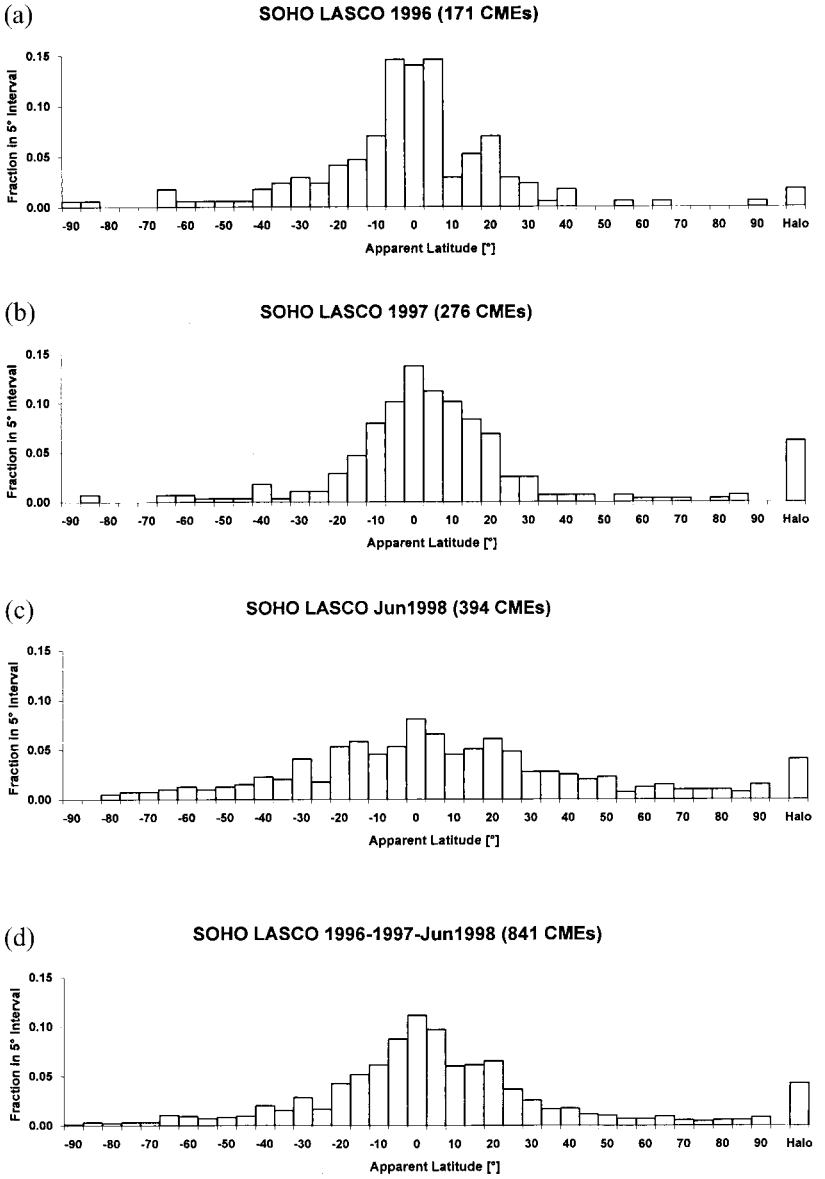

Figure 2. Distribution of Apparent Latitudes. (a–c) The distributions for each calendar year. (d) The cumulative total. "Halo CMEs" span 360° and completely surround the occulting disk, so a location is not assigned for these events.

structures were excluded from that measurement. However, the enhanced sensitivity and dynamic range afforded by LASCO over the earlier instruments allowed the detection of faint extensions on one (or sometimes both) side of some mass ejections that appeared to propagate outward. Such extensions were detected in some 15–20% of the CMEs in this sample, but they have not had a significant effect on the apparent latitude distributions. However, the presence of the extensions to the sides of CMEs has affected the shape of the distribution of apparent sizes of mass ejections by slightly shifting the peak to larger values when compared to earlier results.

Figure 3 shows the plots of apparent angular size, on an annual basis and as a cumulative distribution. These data are asymmetric, with an average apparent size of 72° and a median of 50°. What is striking in these plots compared to earlier reports is the "tail" of events with apparent size larger than ~115°, which had been the (somewhat arbitrary) cutoff in such histograms plotted for Skylab, Solwind, and SMM. These large events comprise ~13% of the total number of CMEs detected by LASCO. If we assume that the earlier instruments would not have detected any of these events, then the average (median) apparent size for the remaining 735 CMEs drops to 47° (45°), which compares rather well to the average values reported by *Hundhausen* [1993] for Skylab (42°) and SMM (47°). However, we believe that the earlier instruments would have detected some fraction of these large CMEs, but we suspect that their apparent size would have been underestimated in instruments with reduced dynamic range. For example, *Burkepile and St. Cyr* [1993] found that only 1.4% of the SMM mass ejections had apparent angular sizes ≥115°. Again, we delay further discussion of the importance of these large CMEs until section 7.

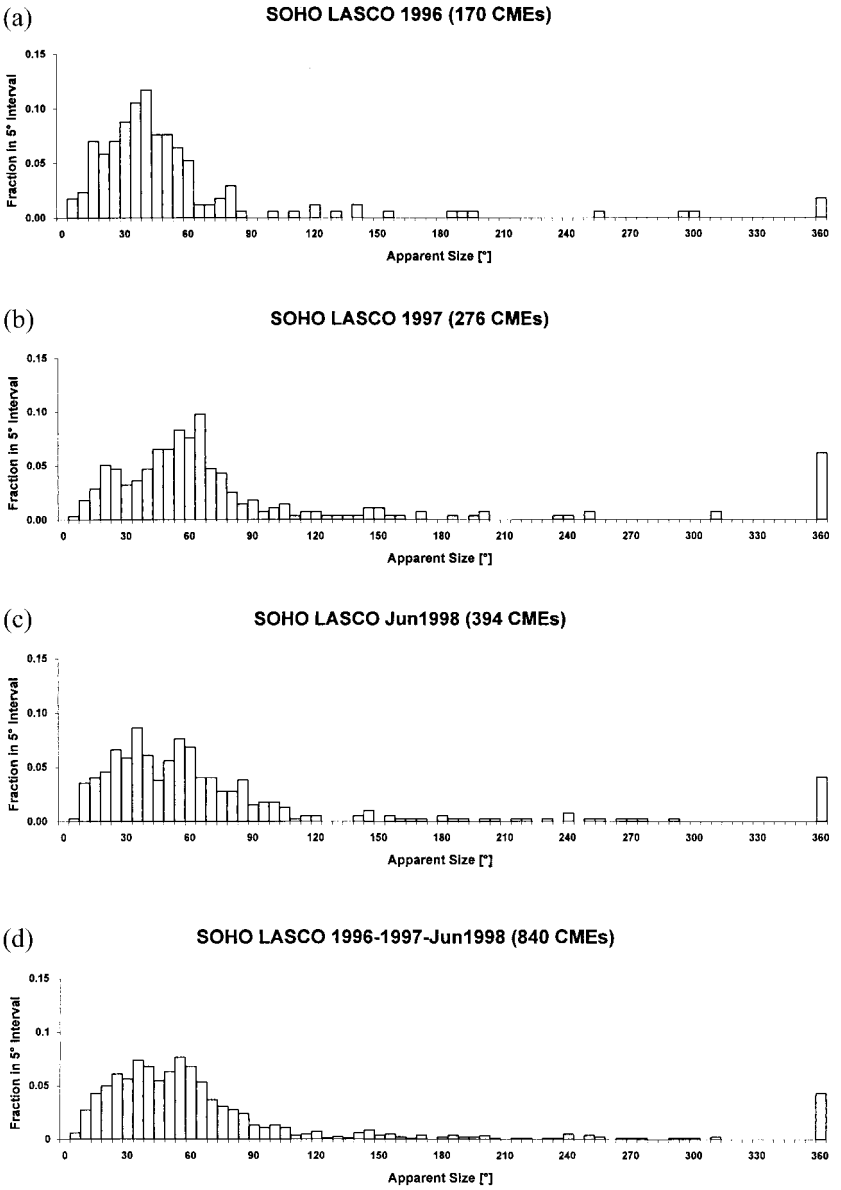

Figure 3. Distribution of Apparent Angular Sizes. (a–c) The distributions for each calendar year. (d) The cumulative total.

6. Apparent Speeds of CMEs

When a morphological feature in a CME could be unambiguously identified in more than a single image, then we were able to measure its height above the solar limb as a function of time and to determine an apparent speed (projected onto the sky plane) for the feature. The reader should be aware that the 30 km/s apparent motion of the Sun across the celestial sphere has not been taken into account in the CME speed measurements. We again stress that all values are apparent and measured as if the Sun were in a fixed position, as has been done for all previous CME work.

We were able to perform a speed measurement for 640/841 (76%) of CMEs in this sample, and this is a significantly larger fraction than the ~50% speed measurements in the Skylab, Solwind, and SMM investigations. We attribute this increase to the greatly expanded field of view afforded by the LASCO C3 and to the ability to observe the Sun continuously without the cyclic interruptions of an Earth-orbiting platform. In 473/640 (74%) of the LASCO speed measurements the feature was identified as the "leading edge" of the CME.

To each height measurement, we assigned an uncertainty based on our ability to distinguish that feature as the contrast decreased (or as the feature evolved) with increasing distance from the Sun. If only two height-time measurements were possible for a given mass ejection, then a simple first-order (constant speed) fit of the data was performed. When more than two measurements were possible we also examined a second-order (constant acceleration) least squares fit of the height-time data, but we rejected the higher-order polynomial fit if the constant speed solution passed through all the measured points or their error bars. The second-order fit was deemed appropriate for 17% of the CMEs in our sample, and this value is comparable to the fraction found for SMM. This is the same data reduction method described by *Hundhausen et*

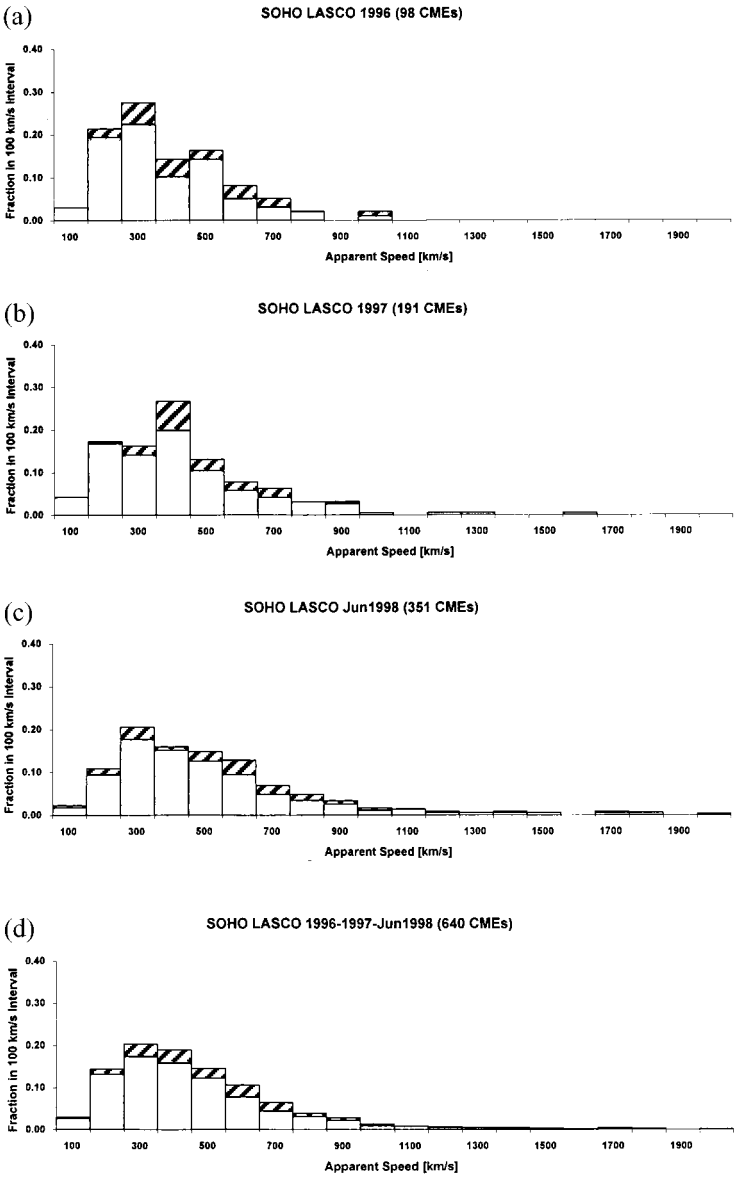

Figure 4. Distribution of Apparent Speeds. (a–c) The distributions for each calendar year. (d) The cumulative total. The fraction of CMEs with constant speeds is shown as the space below the cross-hatched bar; the fraction of CMEs with constant acceleration is shown as cross-hatched.

al. [1994] and *St. Cyr et al*. [1999]; however, on the basis of much of the same data set used here, *Sheeley et al*. [1999] have found a higher fraction of accelerating CMEs using a different technique. Also, *Tappin and Simnett* [1997] and *Srivastava et al*. [1999] have examined cases of CME acceleration in LASCO. We will return to this topic and comment further in section 8.

The distributions of apparent speeds of LASCO CMEs are shown in Figure 4, again as annual and cumulative totals. The cross-hatched bars represent the CMEs where the second-order (constant acceleration) fit was deemed superior to the linear fit, with the speed being evaluated at the final measured point. The distributions are asymmetric, with a "tail" of higher speed (i.e., >1000 km/s) events appearing during 1997–1998. The average speed for all LASCO CMEs in the sample was 424 km/s, and this value is in agreement with that determined by earlier instrumentation. The standard deviation of this average was 275 km/s, although the median value (as shown Table 2) is more frequently noted in CME studies. The maximum speed measured during this interval was 2080 km/s for the leading edge of a CME on March 31, 1998. When the speeds of only the 473 leading edges of CMEs were considered, the average (median) increased to 458 km/s (392 km/s), again in agreement with earlier reports.

There is, however, a dearth of slow events ($\leq$100 km/s) in LASCO when compared to the earlier coronagraphs. We do not have a completely satisfactory explanation for this, but we note that as a class, the slowest CMEs in the SMM catalogue were events that were ill-defined and difficult to measure. It may be that the improvement in dynamic range in LASCO over the earlier coronagraphs has resulted in better speed measurements for these slow CMEs. An alternate explanation is that this may be an effect of the increased field-of-view of LASCO compared to the earlier results. Since the speed of a CME showing constant acceleration is evaluated at the altitude

of the final measurement in this and in previous studies, then this may result in the relative absence of slow events.

It is interesting to examine the effect of the expanded field-of-view of LASCO as it pertains to the speed measurements of CMEs. In Figure 5 we plot, as a function of calendar date, the apparent heights of the first and final measured points in the speed determinations. Figure 5 then shows the range of heights over which the speed of each CME was measured, for the 640 CMEs where that measurement was possible. Figure 5 demonstrates two aspects of these measurements. First, if we assume that our ability to measure speeds is approximately constant over the time interval shown, then the density of vertical lines in Figure 5 is a rough representation of the CME rate. Second, as mentioned before, our ability to track any given CME depended on the contrast and evolution of the morphological feature. Thus the distribution of final measurements (i.e., the top of each line in Figure 5) tells us something about how those characteristics change as a function of radial distance away from the Sun.

In Figure 6 we show the distribution of the "final" altitude measurements for all 640 CMEs. We interpret this graph as a quantification of our ability to measure CMEs as they leave the vicinity of the Sun and enter the heliosphere. As in Figure 4, we have coded the constant speed (open bar) and constant acceleration (cross-hatched) fractions at each apparent altitude. The largest single bin in the Figure 6 distribution lies at the boundary between the C2 and C3 field of view, indicating that we were unable to track some 17% of the CMEs from C2 into C3. This most frequently occurred because the CME morphology evolved as it passed from C2 to C3 or because the change of spatial scale between the telescopes introduced ambiguity in identification of the feature being tracked, even though we could detect the CME beyond this height.

Beyond $\sim 6\,R_{\rm Sun}$ the distribution in Figure 6 is relatively flat, and the plot indicates that $\sim$50% of the CMEs could be measured to an apparent distance of $14\,R_{\rm Sun}$. Note that the relative percentage of CMEs showing constant acceleration increases with apparent height, demonstrating that one is more likely to measure acceleration for CMEs that can be tracked further in the field of view. This is also evident in Figure 7 where we have plotted the distribution of range of altitudes (i.e., final height minus initial height) in the height-time measurements. The 50% level in Figure 7 is in the $10\,R_{\rm Sun}$ bin, meaning that half the events were tracked over a distance less than $10\,R_{\rm Sun}$ and half were tracked farther than that apparent distance.

Figure 7 shows that one is more likely to detect acceleration if the CME can be tracked over a larger range of altitudes. This is a complementary result to that presented by *St. Cyr et al*. [1999] who demonstrated that the initial acceleration of CMEs was very difficult to measure reliably in either the MLSO 1.1–2.2 $R_{\rm Sun}$ field of view or separately in the SMM 2.0–5.6 $R_{\rm Sun}$ field. The LASCO C2 and C3 fields of view do not permit measurement of the initial acceleration of CMEs, but the combination of height-time measurements for individual CMEs observed by both instruments resulted in a greater detection rate for acceleration.

7. Halo Coronal Mass Ejections and Geomagnetic Storms

The first report of a "halo" coronal mass ejection was made by *Howard et al*. [1982], who described observations of a CME detected by the Solwind coronagraph onboard USAF satellite P78-1 in November 1979. The CME was described as [*Howard et al*., 1982, p. L101] "...a halo of excess brightness completely surrounding the occulting disk and propagating radially outward in all directions from the Sun." Those authors associated the CME with a filament disappearance near central meridian at the time of the CME and with an interplanetary shock detected at Earth several days later. They also noted that this was an indication of the three-dimensional nature of the CME phenomenon. Observation of the event by Helios was also reported by *Jackson* [1985]. The Solwind instrument detected a few tens of similar events during its operational period (1979–1985). An analysis of interplanetary shocks and low-frequency radio emissions provided additional evidence that some Solwind halo CMEs may have been Earth-directed [*Cane et al*., 1987].

The interpretation of the halo CME as lying out of the plane of the sky and being Earth-directed was questioned by *St. Cyr and Hundhausen* [1988] on the basis of the lack of that type of CME in SMM observations. Those authors suggested that deflections of existing coronal features toward the plane of the sky might lead to the halo morphology.

Throughout the SOHO era, LASCO C2 and C3 have also detected halo CMEs; and the interpretation that at least some of these events have significant components lying far from the plane of the sky (hence may lie along the Sun-Earth line) appears to be correct. We base this conclusion on three separate pieces of evidence:

1. The first piece of evidence is persistence of activity. During quiet times (i.e., solar activity minimum conditions) as were present during much of 1996–1997, one could observe the progression of a magnetically active solar longitude (either active region or filament channel) as solar rotation carried it from the east limb, across central meridian, to the west limb. When the active longitude was near one of the limbs, associated CMEs were of typical (i.e., $\sim$50°) spans. However, when the active longitude was near central meridian, halo CME events associated with specific activity in the low corona were detected. A particularly good example of this behavior was the May 1997 transit of AR 8038, which produced the halo CME documented by *Plunkett et al*. [1998a] as it transited the Northern Hemisphere of the Sun.

2. The second piece of evidence is polarization analysis. *Paswaters et al*. [1998] presented a preliminary analysis of two halo events that coincidentally appeared during the daily polarization sequences (CMEs of January 25, 1998, and April 29, 1998). Although the CMEs were clearly visible in the total intensity images, they could not be detected in the polarized brightness images. We believe this is explained by another aspect of Thomson scattering whereby the scattering function for polarized brightness peaks for a coronal feature near the plane of the sky but drops off sharply for angular displacements of more than 25° from the sky plane [e.g., *Billings*, 1966; *Hundhausen*, 1993].

3. The third piece of evidence is signatures of other forms of associated activity. The locations of several halo CMEs have been identified low in the corona based on observations from Yohkoh and from ground-based data [*Webb et al*., 1998] and from the Extreme ultraviolet Imaging Telescope (EIT [*Delaboudiniere et al*., 1995]) on SOHO [*Thompson et al*., 1998, 1999a].

There were 36/841 (4%) CMEs where the brightness was considered to encircle the occulting disk completely, and, as noted in section 5, these complete halos represent a subset of

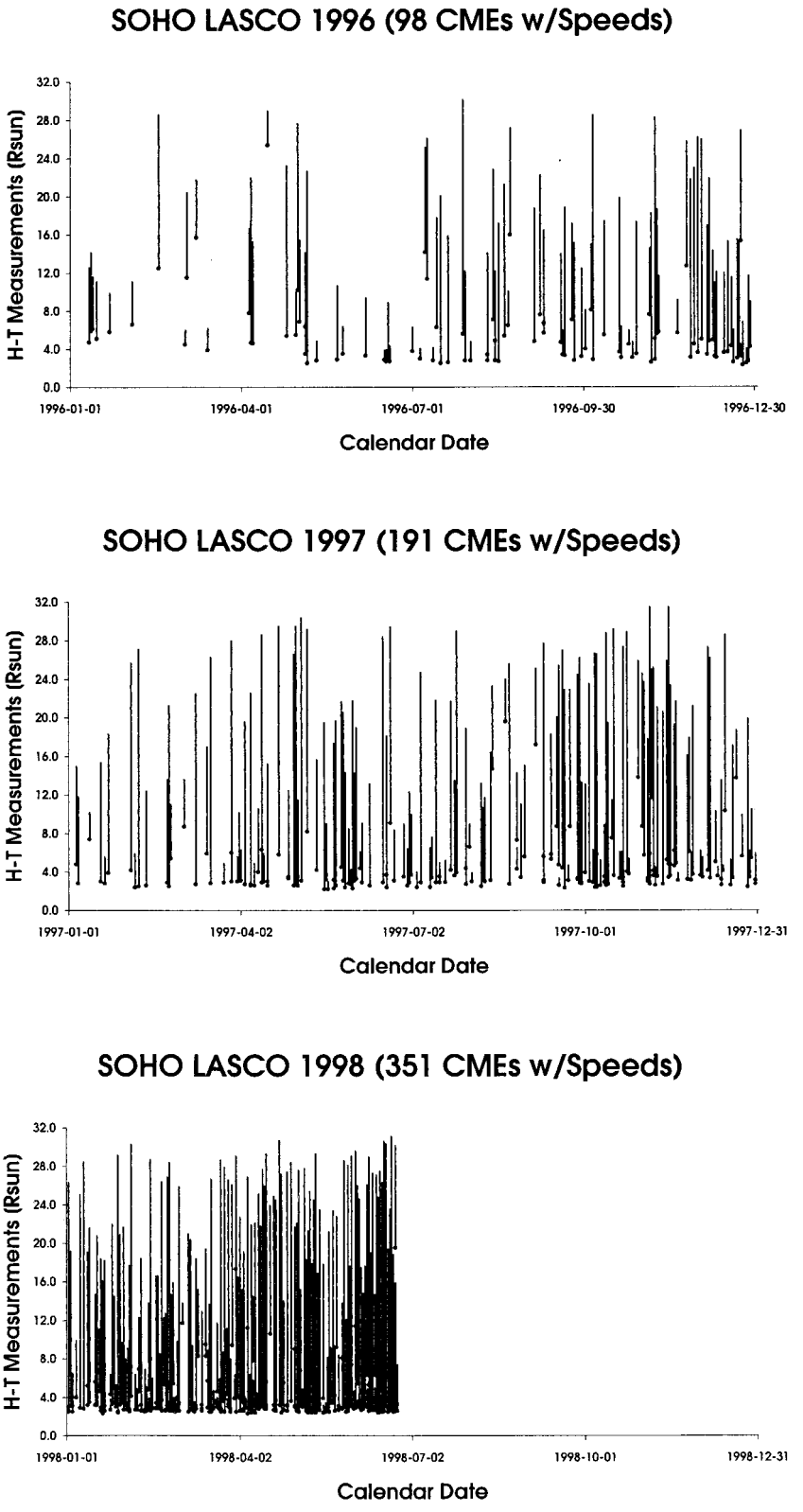

Figure 5. Height-time measurements versus calendar date shown for each of the 3 years covered. The length of each vertical line represents the range of altitudes over which height-time (speed) measurements were made for each event. The overall density of lines gives a sense of the CME rate but is uncorrected for duty cycle.

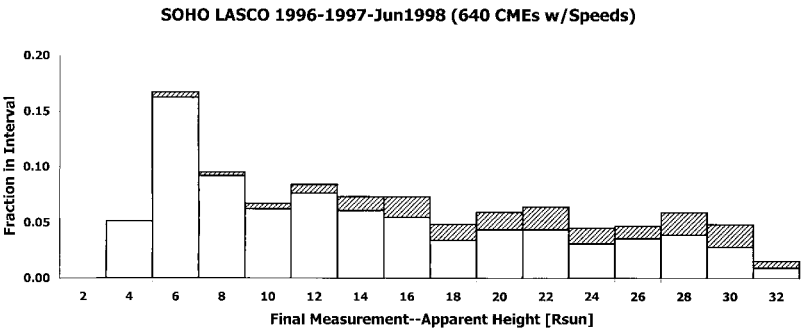

Figure 6. Distribution of "final" altitudes in height-time measurements. This is an indirect method of quantifying the relative brightness of CMEs in this study, since (typically) a brighter event can be measured to greater altitudes. The fraction of CMEs with constant speeds is shown as the space below the cross-hatched bar; the fraction of CMEs with constant acceleration is shown as cross-hatched.

the 13% of LASCO CMEs that span large (≥115°) apparent angles. Plausibility arguments that these events are directed toward (and away from) the Earth based on average CME spans have been presented by *Thompson et al*. [1999b] and *Webb et al*. [1999].

While this might be a convenient place to end the description of halo CMEs, it is instructive to examine this topic further in the spirit of applied science. Although there are several solar sources of geomagnetic activity, most researchers believe that severe geomagnetic storms are the result of CMEs impacting the Earth's magnetosphere [e.g., *McAllister and Crooker*, 1997]. Hence it seems reasonable to examine the record to see if the detection of halo CME events can be used as a predictor of severe geomagnetic activity.

The first issue to address concerns identification of the location of a halo CME. Because the Thomson scattering geometry is symmetric with respect to the plane of the sky (at least to first order), the appearance of a halo CME might indicate that the event was directed toward the Earth (i.e., a frontside event) or it might be directed away from the Earth (a backside event). We believe that in most cases, EUV signatures in the low corona appear to resolve this ambiguity satisfactorily, at least during the era of observations described here. The remainder of our discussion will focus on using only SOHO observations (LASCO C2/C3 and EIT) as a warning system for notification of Earth-directed coronal mass ejections. In fact, this has been done routinely since early 1997 when one of us (D.J.M.) notified a gathering of researchers (at an International Solar-Terrestrial Physics workshop) that a halo CME had been sighted on January 6, 1997, in LASCO C2/C3 observations. Although there were no EIT observations available for that event, the resulting geomagnetic, research [e.g., *Fox et al*., 1998], and public relations activities have led to an anecdotal belief that instrumentation similar to LASCO and EIT might be sufficient to predict geomagnetic activity. One goal of this manuscript is to quantify that ability on the basis of the archive of existing observations so that researchers and policy-makers can assess the benefits of such an observing system.

Beginning in May 1996, the nominal sequence of images obtained by EIT included a full set of synoptic images every 6 hours (304 Å (He II), 171 Å (Fe IX-X), 195 Å (Fe XII), and 284 Å (Fe XV)), along with reduced resolution 195 Å images every 2 hours as part of a "CME Watch" program. After the acquisition of additional telemetry again in April 1997, the cadence and the spatial resolution of 195 Å images increased to several per hour. One can examine EIT images from any of these data sets to look for other solar activity associated with the appearance of a coronal mass ejections, including flares and newly appearing loops in active regions, stable and erupting filaments (and prominences) in absorption and in emission, transient disturbances (e.g., waves) and coronal dimmings over large areas, deflections of preexisting coronal features, and arcade formations. A description of many of these signatures is given by *Thompson et al*. [1999b]. Specific examples of Earth-

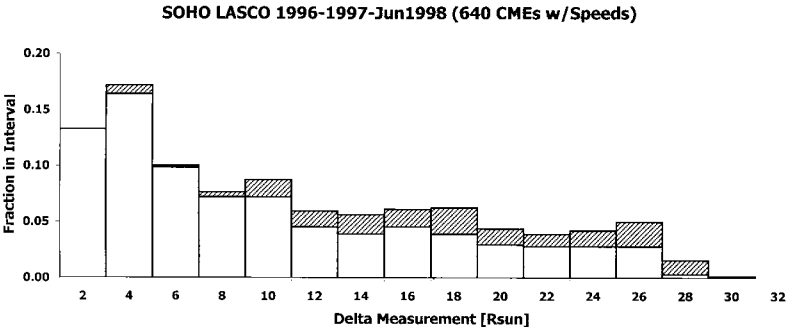

Figure 7. Distribution of the range of altitudes in height-time measurements. This is an indirect method of quantifying the relative brightness of CMEs in this study, since (typically) a brighter event can be measured over a greater range of altitudes. The fraction of CMEs with constant speeds is shown as the space below the cross-hatched bar; the fraction of CMEs with constant acceleration is shown as cross-hatched. Half of the CMEs were tracked over a range of $\sim 10\ R_{\mathrm{Sun}}$.

Table 3. Annual and Cumulative Statistics for SOHO LASCO and EIT Halo CMEs

	1996 (Partial) Begins May 1, 1996	1997	1998 (Partial) Ends June 30, 1998	Total
LASCO Halo CMEs	12	37	43	92
EIT Front	2	14	15	31*
EIT Front?	1	4	4	9*
EIT Back	1	6	13	20
EIT Back?	8	11	5	24
EIT Data Gap	0	2	6	8

LASCO C2/C3 halo CMEs; defined as width ≥120 and cross central meridian longitude projection. Determination of frontside versus backside from EIT images.

*40 SOHO LASCO/EIT potential SWx events.

directed (frontside) events have been provided by *Burlaga et al*. [1998], *Webb et al*. [1998], *Thompson et al*. [1998], and *Plunkett et al*. [1998]; and links between geomagnetic storms and LASCO halo events have been reported by *Brueckner et al*. [1998] and *Webb et al*. [1999].

A second issue concerns the distribution shown in Figure 3, which demonstrated that the apparent sizes for CMEs may be any angular width up to and including 360°. If the white light emission in a halo CME is due to the same scattering mechanism/geometry as the well-known limb events (i.e., there are no deflections of preexisting features) and if the average longitudinal width of CMEs is equal to the average latitudinal width, then CMEs with apparent sizes less than 360° may also have a component that could strike the Earth. Unfortunately, there is no direct information about the longitudinal extent of coronal mass ejections, but indirect methods suggest that the in-ecliptic size may be comparable to the measured latitudinal span, at least for the few cases where such an estimate has been possible [e.g., *Fisher and Munro*, 1984]. There are also indications from in situ measurements that the longitudinal extent of interplanetary CMEs may be even larger than the apparent latitudinal widths measured for CMEs [e.g., *Richardson and Cane*, 1993]. Thus it seems reasonable to assume that a CME need not be aligned directly along the Sun-Earth line in order to strike the magnetosphere.

So is there a threshold apparent size for CMEs above which we are assured that a component will strike the Earth and below which we are assured that the CME will miss? *Webb et al*. [1999] used 140° as a threshold and reported good results for the period December 1996 through June 1997. One of their conclusions was that even some of the partial halo CMEs in their sample may be geoeffective when the source region in the low corona is within ~0.5 radii of Sun center.

On the basis of an argument presented by *Thompson et al*. [1999b], the operations staff of LASCO and EIT used the following criteria for halo CME alerts: the CME must have an apparent size larger than 120°, and some portion of the CME must appear to intersect position angle 0° or 180° (i.e., it must cross the projection of either the Sun's north or south pole). Invoking these two criteria eliminated almost 89% of the CMEs in this sample, resulting in 92 complete and partial halos in 841 CMEs. We direct the reader to Table 3, where we show the annual and cumulative statistics of these CMEs.

In Table 3 we further categorize each halo CME according to the EIT observations available at the time of the appearance of the event. (We have extended the duration of the time frame up to June 30, 1998, to allow travel time for any disturbance leaving the Sun prior to the June 24 cessation of operations.) As described above, some events were clearly visible in the EIT observations in the low corona, based on reasonable temporal and spatial constraints for association, and those are identified as "EIT Front." The category "EIT Front?" was assigned when activity was detected but either the cadence of images made the association less convincing, multiple events were in progress, or temporal and spatial requirements had to be relaxed to make the association. Some events were clearly detected in projection (behind the limb) in EIT images, so those were categorized as "EIT Back." Finally, when nothing was detected in EIT but the cadence and coverage seemed adequate to identify CMEs, we assumed the event was backside and categorized it "EIT Back?." For a few events (including the well-known January 6, 1997, halo), no EIT data were available ("EIT Data Gap").

On the basis of only LASCO C2/C3 and EIT, we found that 40 of the 92 halo CMEs might be Earth-directed. Since there were 8/92 cases that were indeterminate (EIT data gaps), this yields 40/84 (48%) that were apparently frontside. This value seems reasonable considering reports from an earlier solar cycle suggesting that the interplanetary CME rate at Earth was 12 CMEs/year during activity minimum and as many as ~72 CMEs/year during activity maximum conditions [*Gosling et al*., 1992].

Although we risk ignoring much very interesting physics, we can investigate the activity of the geomagnetic field over this same 25 month period to determine the utility of SOHO LASCO/EIT halo CMEs as predictors of *Kp* storms. Table 4 shows the results of this comparison, where we first tabulate the number of severe (defined as $Kp \geq 6$ for any interval) geomagnetic storms. There were 21 severe geomagnetic storms during this interval. We have examined how many of those storms could be associated, assuming some reasonable travel time from the Sun to the Earth, with any of the SOHO LASCO/EIT frontside halo CMEs. We found that 15/21 (71%) appeared within 60–138 hours following the first appearance of one of the 40 frontside halo events. This time duration corresponds to average speeds of 300–700 km/s for the 1 AU travel distance, and this time frame was chosen to match the range of solar wind speeds typically sampled at the Earth. (Figure 4 showed a wider distribution of apparent speeds for CMEs measured near the Sun. However, we will not speculate here about the accommodation of those high-speed CMEs into the solar wind flow since that process apparently occurs outside of the LASCO C3 32 R_{Sun} field of view.)

Six of the severe geomagnetic storms during this interval did not have obvious coronal counterparts, and these were considered "LASCO/EIT misses" because they would not have been predicted using the SOHO instruments. However, three of those six occurred following observational data gaps (two for EIT and one for LASCO). If we eliminate these storms, then as many as 15/18 (83%) of the CMEs causing *Kp* storms were identified by LASCO/EIT several days before they reached the Earth. The bottom section of Table 4 shows the same statistical breakdown for $Kp \geq 5$. Although the absolute number of false alarms decreases, there is an even larger fraction of these geomagnetic disturbances that cannot be accounted for by LASCO/EIT halo coronal mass ejections.

In Figure 8 we examine these 15 intervals of $Kp \geq 6$ more closely. Here we show the relationship between delay time (i.e., the length of time between the first detection of the CME in

LASCO and the time of the maximum *Kp*) and the apparent speed of the CME as measured by LASCO. The size of the points indicates the maximum severity of the geomagnetic storm (smallest point is $Kp = 6.0$; largest point is $Kp = 8.7$) and a 10% error in the apparent speed measurements in indicated. The two endpoints of the dashed line show the idealized 1 AU transit time for a 400 km/s (104 hours) and an 800 km/s (52 hours) average speed. We should note that *Kp* is measured in 3 hour intervals, so any timing has at least that granularity. Also, the time of the maximum *Kp* is plotted, but geomagnetic storm levels may have been attained prior to that time or persisted after that time, and this is indicated by the length of the horizontal uncertainties (for $Kp \geq 5$). Further, the time of the first appearance in LASCO means that the CME has already begun its travel toward the Earth and is some unknown distance from the Sun. Finally, a correction to account for the variation in Sun-Earth distance has also not been considered, and that factor could result in an additional uncertainty of about one *Kp* time interval (i.e., ~3.5 hours for a 400 km/s CME between perihelion and aphelion).

Several things are worthy of mention in Figure 8. First, there does not appear to be a clear relationship between the LASCO measurement of CME speed and either the delay time or the *Kp* storm severity. Without knowledge of the actual angular span of a halo CME, then we cannot correct for the significant projection effects in the measurement of apparent speed. *Sheeley et al*. [1999] offer one possibility for determining "fast" versus "slowly accelerated" halo CMEs; and there may be other noncoronagraphic methods to determine the actual CME span (e.g., the size of the coronal dimming region in EIT). However, as of this writing, the LASCO apparent speed measurement for halo CMEs must be viewed with caution.

Second, if the association between the individual *Kp* storms and the LASCO/EIT CMEs is correct, then some of the CMEs have been slowed in their transit from the Sun to the Earth. We already mentioned the uncertainty in our knowledge of the radial distance from the Sun at the time the CME was first detected in LASCO, but this would not account for the dispersion in Figure 8.

The level of geomagnetic forecast demonstrated in this simple statistical analysis using LASCO/EIT exceeds that reported by present methods [e.g., *Joselyn*, 1995]. Of course, there are actually other remote and in situ observations that are used by forecasters and by researchers to form a more complete description of any single event [e.g., *St. Cyr and Webb*, 1991; *Kaiser et al*., 1998; *Hudson et al*., 1998; *Cane et al*., 1998], and new methods are being examined [e.g., *Luhmann et al*., 1998]. However, we believe that the results presented here using only full-disk EUV imaging and white light coronagraphs are quite remarkable.

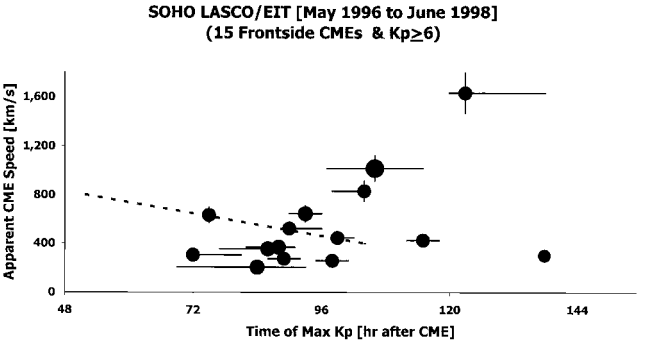

Figure 8. Delay time between maximum *Kp* value and CME detection versus apparent speed measurement of CME by LASCO. The size of the dots indicates the severity of the *Kp* storm (smallest dot is $Kp = 6.0$; largest dot is $Kp = 8.7$). A 10% uncertainty in speed measurement is shown pro forma (see text discussion). Uncertainties in the time axis represent the duration where *Kp* remained above storm values (i.e., $Kp = 5$). The endpoints of the dashed line show the travel time for a disturbance leaving the Sun at 400 km/s (104 hours) and 800 km/s (52 hours).

However, there are certainly several issues to address concerning this method, and many of these will be the topic of future reports. First, predictions of three $Kp \geq 6$ storms were apparently missed completely, and reexamination of the LASCO/EIT data did not reveal noteworthy events. Second the method generated "false alarms" since 40 "alerts" were produced, yet (at best) only 15 storms were correctly forecast. Third the dispersion in travel times between the LASCO/EIT observation and the appearance of the *Kp* storm is likely too large to be of practical use to a space weather forecaster (note, of course, that forecasters have other resources beyond those used in this study). Fourth, a recent report by *Sheeley et al*.

Table 4. Annual and Cumulative Statistics for *Kp* Versus SOHO LASCO and EIT Halo CMEs

	1996 (partial) Begins May 1, 1996	1997	1998 (partial) Ends June 30, 1998	Total
Annual Tabulation of Kp *Storms ≥6 Compared to LASCO/EIT Observations*				
$Kp \geq 6$ ("severe")	2	11	8	21 periods $Kp \geq 6$
LASCO/EIT frontside halo CME	1	8	6	15 LASCO/EIT frontside halo CMEs
LASCO/EIT miss	1	3	2	6 LASCO/EIT misses (three data gaps)
LASCO halo; EIT data gap	···	1	1	
LASCO data gap	···	···	1	
LASCO/EIT false alarms	2	10	13	25 LASCO/EIT false alarms 8 LASCO halos—EIT data gap
Annual Tabulation of Kp *Storms ≥5 Compared to LASCO/EIT Observations*				
$Kp \geq 5$	11	20	12	43 periods $Kp \geq 5$
LASCO/EIT frontside halo CME	1	12	7	20 LASCO/EIT frontside halo CMEs
LASCO/EIT miss	10	8	5	23 LASCO/EIT misses (three data gaps)
LASCO halo; EIT data gap	···	1	1	
LASCO data gap	···	···	1	
LASCO/EIT false alarms	2	6	12	20 LASCO/EIT false alarms 8 LASCO halos—EIT data gap

[2000] described several examples of high-speed CMEs that were associated with EIT events at or near the limb. These CMEs produced halo-like deflections that surrounded the LASCO occulting disk, similar to the manner suggested by *St. Cyr and Hundhausen* [1987]. As of this writing the LASCO/EIT operations teams at Goddard and at Naval Research Laboratory (NRL) continue to provide warnings of potential Earth-directed CMEs, typically within 24 hours of the event at the Sun. We continue to examine different aspects of the LASCO/EIT observations in an effort to understand their utility as geomagnetic storm predictors.

8. Discussion

In the preceding text we have attempted to include discussion with each topic as it appeared. However, there are additional comments and brief observations that are relevant to the coronal mass ejection observations of LASCO, and we consider those topics here.

8.1. Identification of CMEs

St. Cyr et al. [1999] reported that virtually all of the CMEs detected in data from the ground-based MK3 telescope observations of the inner corona were also seen in the middle corona, when observations from SMM were available. However, they were unable to account for all SMM mass ejections that appeared during the MK3 observing window but were not seen by MK3. They attributed this to several possibilities (including the difference of observing the coronal polarization brightness versus total brightness), but they left open the possibility that some mass ejections may form at altitudes above the MK3 field of view ($\sim$2.0 $R_{\rm Sun}$).

With LASCO we have another opportunity to test this question over different fields of view. Specifically, were all mass ejections identified in the data detected in both C2 and C3? When adequate data coverage was available for both telescopes (which was most of the time), almost all mass ejections were detected by both telescopes. Exceptions to that statement can be made for the following cases: (1) some weak CMEs appeared in C2, but were not readily detectable in C3. This was evident in the discussion of Figure 6, where we noted that some events could not be tracked from C2 into C3. (2) Some events appeared to be multiple (i.e., separate) CMEs in C2, but they appeared to merge into a single front in C3 after $\sim$10 $R_{\rm Sun}$. This was difficult to quantify since individual observers used different criteria as to what constituted "merging"; hence this topic requires further examination in the future. However, we identified no CMEs appearing solely in C3. Thus there does not appear to be a population of coronal mass ejections that originate at altitudes above $\sim$4 $R_{\rm Sun}$.

We are aware of several events imaged in emission lines in the low corona by EIT where (apparently) chromospheric material was ejected from distinct, multiple heliographic latitudes and longitudes near one of the limbs (e.g., September 23–24, 1997). However, when that ejected material appeared in C2/C3, it appeared as a single mass ejection. Therefore, as we stated in section 1, to maintain comparability with previous compilations of white light CMEs, we have ignored this additional information and compiled these events as single CMEs. This may be undesirable (and is likely even incorrect) from the standpoint of understanding cause and effect in CMEs, and there is work in progress to examine and to report on the statistics of combined LASCO and EIT CME observations [*Thompson et al*., 1999b; S. P. Plunkett et al., New insights on coronal mass ejections from SOHO, submitted to *Advances in Space Research*, 1998]. However, as of this writing, we choose to report on the LASCO observations of CMEs alone.

8.2. CME Acceleration and Deceleration

For the 17% of CMEs with measured speeds where acceleration was reliably detected, the values ranged from 1.4 m/s^2 to 49.1 m/s^2 with an average (median) of 9.6 m/s^2 (6.9 m/s^2). As described in section 6, these represent an average constant acceleration over the fraction of the C2/C3 fields of view where the measurements were obtained. These values constitute only a small portion of the range of accelerations reported by *St. Cyr et al*. [1999] on the basis of combining SMM data with ground-based MLSO measurements of CMEs in the inner corona (below 1.5 $R_{\rm Sun}$). The LASCO result emphasizes the importance of obtaining measurements of the CME in the inner corona, where the force(s) acting on it lead to its formation, initial expansion, and initial acceleration.

Some striking examples of material accelerating and decelerating through the C2/C3 fields have been shown by *Sheeley et al*. [1999]. However, the technique described in that report is significantly different from that employed in this manuscript or in the earlier reports. Further work will be necessary to understand the differences between these two methods.

Deceleration was not detected in any of the CMEs in this sample. However, some 51/640 (8%) were traveling with speeds of 800 km/s or greater through C2 and C3, and we know that in situ measurements rarely (if ever) detect solar wind speeds of this magnitude in the interplanetary medium. The material comprising these mass ejections must be decelerated outside of the C3 field of view, and the answer to that question is not resolved by these observations.

8.3. Nonradial Motions

In the inner corona, nonradial motions have been reported by *Plunkett et al*. [1998b] as a characteristic of the location of EIT activity associated with LASCO CMEs. *Harrison* [1986] noted the offset of associated X-ray activity away from the central axis of SMM coronal mass ejections, but *St. Cyr et al*. [1999] did not find a significant fraction of the MLSO-SMM CMEs displaying nonradial motion. This quality has not been measured rigorously during this compilation of LASCO CMEs; however, particularly noteworthy cases of CME motion off a strictly radial trajectory were noted. A tally of the number of events showing this characteristic follows: 1996, 14 CMEs; 1997, 23 CMEs; 1998, 81 CMEs; Total, 118 events (118/841 = 14%). This is likely a lower limit since only events with significant (i.e., at least 10°) nonradial motions were noted. However, it indicates that forces other than those resulting in purely radial expansion continue to act on at least this fraction of the CME structures, even at the altitudes covered by LASCO C2/C3.

8.4. Concave-Outward Morphological Features

Illing and Hundhausen [1983] reported the observation of a "concave-outward" morphological structure propagating away from the Sun in 1980 observations of a CME by SMM. The feature appeared late in the formation of the mass ejection, at the apparent trailing edge of the CME, and they interpreted this as potential evidence of a magnetic structure that had become disconnected from the Sun. In the compilation of all SMM events, *Burkepile and St. Cyr* [1993] noted that about 6%

of the mass ejections possessed this morphology. *Webb and Cliver* [1995] examined Skylab, SMM (1980 only), and eclipse data and identified circular or concave-outward features in at least 10% of CMEs. *Simnett et al*. [1997] reported examples of a Y morphology, interpreted as a disconnected magnetic structure with trailing neutral sheet, from LASCO observations; and *Wu et al*. [1997] modeled a similar LASCO event. However, *Wang et al*. [1999] reported their interpretation of two LASCO streamer events as disconnection without the concave-outward morphology.

Chen et al. [1997] found good agreement between a magnetic flux rope model and the morphological shape of a LASCO CME appearing on April 13, 1997. This event was similar to the "circular" shape described by *Webb and Cliver* [1995] in that the trailing edge of the mass ejection could be described as "concave-outward." *Wood et al*. [1999] have found that the kinematic and morphological properties of two LASCO CMEs could be modeled as erupting magnetic flux ropes. Recently, *Dere et al*. [1999] have described three events observed by SOHO LASCO and EIT, and they interpret the concave-outward morphology as the signature of magnetic flux ropes. They estimate the fraction of LASCO CMEs showing such morphology to be 25–50%.

It seems clear that the enhanced dynamic range of LASCO over earlier instrumentation has resulted in the apparent detection of a significantly larger fraction of these concave-outward structures than has previously been reported. The fraction of CMEs that displayed this morphology is shown in Table 5 on an annual basis. Although there is some dispersion in these fractions, we believe that it is significant that at least 36% (and perhaps 48%) of all of the CMEs detected in LASCO showed some kind of concave-outward morphological feature late in the event (i.e., always trailing the leading feature). We have not distinguished between the circular concave-outward features and the "V-shaped" or "Y-shaped" morphology in the accounting reported here. Whether or not all of these shapes are significant evidence of either flux rope geometry or of disconnected magnetic structures is a question that requires further examination. However, we provide this statistic for direct comparison to the much lower fraction reported for SMM [*Burkepile and St. Cyr*, 1993] as an example of an apparent instrumental limitation in the earlier observations.

8.5. CME Expansion

The SOHO LASCO observations (particularly those of C3, the outermost field) contain new information about the evolution of CMEs and about their propagation through and interaction with the interplanetary medium. For example, does the morphology of a mass ejection change as a function of altitude? *Hildner* [1977] found that many CMEs appeared to narrow with altitude (i.e., the span appeared to contract latitudinally) in Skylab coronagraph observations. Using Skylab and SMM observations, *MacQueen and Cole* [1985] found mixed results when they attempted to measure the thickness of the leading edge of CMEs as a function of altitude.

Our preliminary examination indicates that expansion of morphological features is common along the radial direction within any given CME, but expansion (or significant contraction) in the latitudinal direction is rarely, if ever, detected. Plots of the shape of several LASCO CMEs were presented as a function of altitude by *Funsten et al*. [1999], and no significant latitudinal expansion is evident, at least for those events. Radial expansion measurements of some LASCO CMEs have been made for a few events that could be tracked through at least 20 R_{Sun} in the LASCO C3 field [*St. Cyr and Howard*, 1999]. Typical expansion values range from 5 to 20 R_{Sun}/day (or ~0.02–0.10 AU/day). A more detailed, quantitative study of the behavior of LASCO CMEs as a function of altitude is in preparation.

Table 5. Statistics of "Concave-Out" Morphology Appearance in SOHO LASCO CMEs

	1996	1997	1998	Total
Yes	0.23	0.46	0.34	0.36
No	0.62	0.42	0.55	0.52
Maybe	0.15	0.12	0.11	0.12
	100%	100%	100%	100%

Annual fractions and total fraction of CMEs with "concave-out" morphology.

9. Conclusions

Perhaps the most remarkable conclusion of the study presented here is that in spite of the enhanced brightness sensitivity and superior stray light reduction of the SOHO LASCO coronagraphs over previous instrumentation, the fundamental statistical measures of coronal mass ejections have not been altered substantially. In this report we have described the results of a thorough survey of coronal mass ejections observed by the SOHO LASCO C2 and C3 white-light coronagraphs from January 1996 through June 1998. The analysis of these data has, to the extent possible, been executed in the same manner as was done in previous studies so that meaningful comparisons could be drawn. We briefly summarize our conclusions as follows: (1) We did not detect a significant number of low-mass (i.e., faint) events; nor did we find a class of CME that originates high in the corona. (2) A preliminary visibility function analysis based on Type II radio bursts indicates that LASCO C2 and C3 detected virtually all CMEs. (3) The magnitude and phase of the CME rate, as well as the distribution of apparent locations, varied in the manner expected. (4) The distribution of apparent speeds and the accelerations were as expected. (5) The general shape of the distribution of apparent sizes for LASCO CMEs is similar to those of earlier reports, but the average apparent size (72°) is larger due to at least some events with significant longitudinal components directed along the Sun-Earth line (the halo events). (6) There were 92 complete and partial halos in the 841 CMEs. Using full disk solar images obtained at extreme ultraviolet wavelengths from EIT on SOHO, we found that 40/92 of these events might have been directed toward the Earth, and we compared the timing of those with the *Kp* geomagnetic storm index in the days following the CME. Although the "false alarm" rate was high, we found that 15/21 (71%) of the $Kp \geq 6$ storms could be accounted for as SOHO LASCO/EIT frontside halo CMEs. Elimination of three *Kp* storms that occurred after SOHO data gaps increases the fraction detected to 15/18 (83%).

Acknowledgments. The late G. E. Brueckner was the principal investigator for LASCO during the development and operational phases during which these observations were obtained. Significant software contributions to the program were made by D. Wang of Interferometrics at NRL. Operations expertise was provided by E. Einfalt, S. Stezelberger, and K. Schenk. Additional support has been provided by R. Duffin, N. Rich, J. Desselle, and L. Gould. The SOHO LASCO

operations and data analysis have been supported by NASA contract S-86760-E. One of us (O.C.S.) wishes to acknowledge useful discussions and suggestions by H. V. Cane, J. T. Burkepile, and the two referees. One of us (O.C.S.) wishes to acknowledge partial support by the National Space Weather Program under NSF grant ATM-9819668. One of us (N.R.S.) received financial support from the Office of Naval Research/NRL Research Option "Solar Magnetism and the Earth's Environment" and from NASA. One of us (D.F.W.) wishes to acknowledge support by AFOSR grant AF49620-91-1-0062. SOHO is a mission of international cooperation between the European Space Agency and NASA.

Janet G. Luhman thanks Bernard V. Jackson and another referee for their assistance in evaluating this paper.

References

Billings, D. E., *A Guide to the Solar Corona*, Academic Press, New York, 1966.

Brueckner, G. E., et al., The large angle spectroscopic coronagraph (LASCO), *Sol. Phys*., *162*, 357–402, 1995.

Brueckner, G. E., J.-P. Delaboudiniere, R. A. Howard, S. E. Paswaters, O. C. St. Cyr, R. Schwenn, P. Lamy, G. M. Simnett, B. Thompson, and D. Wang, Geomagnetic storms caused by coronal mass ejections (CMEs): March 1996 through June 1997, *Geophys. Res. Lett*., *25*, 3019–3022, 1998.

Burkepile, J. T., and O. C. St. Cyr, A revised and expanded catalogue of coronal mass ejections observed by the *Solar Maximum Mission* coronagraph, *NCAR Tech. Note TN-369+STR*, Natl. Cent. Atmos. Res., Boulder, Colo., 1993.

Burlaga, L., et al., A magnetic cloud containing prominence material: January 1997, *J. Geophys. Res*., *103*, 277–285, 1998.

Cane, H. V., N. R. Sheeley, and R. A. Howard, Energetic interplanetary shocks, radio emission, and coronal mass ejections, *J. Geophys. Res*., *92*, 9869–9874, 1987.

Cane, H. V., I. G. Richardson, and O. C. St. Cyr, The interplanetary events of January–May, 1997 as inferred from energetic particle data, and their relationship with solar events, *Geophys. Res. Lett*., *25*, 2517–2520, 1998.

Chen, J., R. A. Howard, G. E. Brueckner, R. Santoro, J. Krall, S. E. Paswaters, O. C. St. Cyr, R. Schwenn, P. Lamy, and G. M. Simnett, Evidence of an erupting magnetic flux rope: LASCO coronal mass ejection of 1997 April 13, *Astrophys. J*., *490*, L191–L194, 1997.

Cliver, E. W., O. C. St. Cyr, R. A. Howard, and P. S. McIntosh, Rotation-averaged rates of coronal mass ejections and dynamics of polar crown filaments, in *Solar Coronal Structures*, edited by V. Rusin, P. Heinzel, and J.-C. Vial, pp. 83–90, Veda Publ. House of the Slovak Acad. of Sci., Bratislava, Slovakia, 1994.

Cliver, E., N. Gopalswamy, R. Howard, C. St. Cyr, and D. Webb, Metric Type II bursts and CMEs during the SOHO mission, *Eos Trans. AGU*, *79*(46), Fall Meet. Suppl., F712, 1998.

Delaboudiniere, J.-P., et al., EIT: Extreme-ultraviolet imaging telescope for the SOHO mission, *Sol. Phys*., *162*, 291–312, 1995.

Dere, K. P., et al., EIT and LASCO observations of the initiation of a coronal mass ejection, *Sol. Phys*., *175*, 601–612, 1997.

Dere, K. P., G. E. Brueckner, R. A. Howard, D. J. Michels, and J.-P. Delaboudiniere, LASCO and EIT observations of helical structure in coronal mass ejections, *Astrophys. J*., *516*, 465–474, 1999.

Domingo, V., B. Fleck, and A. I. Poland, The SOHO mission: An overview, *Sol. Phys*., *162*, 1–37, 1995.

Fisher, R. R., and R. H. Munro, Coronal transient geometry, I, The flare-associated event of 1981 March 25, *Astrophys. J*., *280*, 428–439, 1984.

Fox, N. J., M. Peredo, and B. J. Thompson, Cradle to grave tracking of the January 6–11, 1997 Sun-Earth connection event, *Geophys. Res. Lett*., *25*, 2461–2464, 1998.

Funsten, H. O., J. T. Gosling, P. Riley, O. C. St. Cyr, R. J. Forsyth, R. A. Howard, and R. Schwenn, Combined Ulysses solar wind and SOHO coronal observations of several west limb coronal mass ejections, *J. Geophys. Res*., *104*, 6679–6689, 1999.

Gosling, J. T., The solar flare myth, *J. Geophys. Res*., *98*, 18,937–18,949, 1993.

Gosling, J. T., Coronal mass ejections, in *26th International Cosmic Ray Conference Invited, Rapporteur, and Highlight Papers*, edited by B. Dingus, D. Kieda, and M. Salamon, in press, 1999.

Gosling, J. T., D. J. McComas, J. L. Phillips, and S. J. Bame, Counterstreaming solar wind halo electron events: Solar cycle variations, *J. Geophys. Res*., *97*, 6531–6535, 1992.

Harrison, R. A., Solar coronal mass ejections and flares, *Astron. Astrophys*., *162*, 283–291, 1986.

Harvey, K. L., and O. R. White, What is solar cycle minimum?, *J. Geophys. Res*., *104*, 19,759–19,764, 1999.

Hildner, E., Mass ejections from the solar corona into interplanetary space, in *Study of Travelling Interplanetary Phenomena*, edited by M. A. Shea et al., pp. 3–21, D. Reidel, Norwell, Mass., 1977.

Howard, R. A., D. J. Michels, N. R. Sheeley Jr., and M. J. Koomen, The observation of a coronal transient directed at Earth, *Astrophys. J*., *263*, L101–L104, 1982.

Howard, R. A., N. R. Sheeley Jr., M. J. Koomen, and D. J. Michels, Coronal mass ejections: 1979–1981, *J. Geophys. Res*., *90*, 8173–8191, 1985.

Hudson, H. S., J. R. Lemen, O. C. St. Cyr, A. C. Sterling, and D. F. Webb, X-ray coronal changes during halo CMEs, *Geophys. Res. Lett*., *25*, 2481–2484, 1998.

Hundhausen, A. J., Sizes and locations of coronal mass ejections: SMM observations from 1980 and 1984–1989, *J. Geophys. Res*., *98*, 13,177–13,200, 1993.

Hundhausen, A. J., Coronal mass ejections, in *The Many Faces of the Sun*, edited by K. T. Strong et al., pp. 143–200, Springer-Verlag, New York, 1999.

Hundhausen, A. J., C. B. Sawyer, L. House, R. M. E. Illing, and W. J. Wagner, Coronal mass ejections observed during the Solar Maximum Mission: Latitude distribution and rate of occurrence, *J. Geophys. Res*., *89*, 2639–2646, 1984.

Hundhausen, A. J., J. T. Burkepile, and O. C. St. Cyr, Speeds of coronal mass ejections: SMM observations from 1980 and 1984–1989, *J. Geophys. Res*., *99*, 6543–6552, 1994.

Illing, R. M. E., and A. J. Hundhausen, Possible observation of a disconnected magnetic structure in a coronal transient, *J. Geophys. Res*., *88*, 10,210–10,214, 1983.

Jackson, B. V., Helios observations of the Earthward-directed mass ejection of 27 November, 1979, *Sol. Phys*., *95*, 363–370, 1985.

Jackson, B. V., and R. A. Howard, A CME mass distribution derived from Solwind coronagraph observations, *Sol. Phys*., *148*, 359–370, 1993.

Jackson, B. V., and D. F. Webb, The masses of CMEs measured in the inner heliosphere, *Eur. Space Agency Spec. Publ*., *ESA SP-373*, 233–238, 1994.

Joselyn, J. A., Geomagnetic activity forecasting: The state of the art, *Rev. Geophys*., *33*, 383–401, 1995.

Kaiser, M. L., M. J. Reiner, N. Gopalswamy, R. A. Howard, O. C. St. Cyr, B. J. Thompson, and J.-L. Bougeret, Type II radio emissions in the frequency range from 1–14 MHz associated with the April 7, 1997 solar event, *Geophys. Res. Lett*., *25*, 2501–2504, 1998.

Luhmann, J. G., J. T. Gosling, J. T. Hoeksema, and X. Zhao, The relationship between large-scale solar magnetic field evolution and coronal mass ejections, *J. Geophys. Res*., *103*, 6585–6593, 1998.

MacQueen, R. M., and D. M. Cole, Broadening of looplike solar coronal transients, *Astrophys. J*., *299*, 526–535, 1985.

MacQueen, R. M., J. T. Gosling, E. Hildner, R. H. Munro, A. I. Poland, and C. L. Ross, Initial results from the High Altitude Observatory white light coronagraph on *Skylab*: A progress report, *Phil. Trans. R. Soc. London*, *281*, 405–414, 1976.

McAllister, A. H., and N. U. Crooker, Coronal mass ejections, corotating interaction regions, and geomagnetic storms, in *Coronal Mass Ejections*, *Geophys. Monogr. Ser*., vol. 99, edited by N. U. Crooker, J. A. Joselyn, and J. Feynman, pp. 279–289, AGU, Washington, D. C., 1997.

Moses, D., et al., EIT observations of the extreme ultraviolet Sun, *Sol. Phys*., *175*, 571–599, 1997.

Munro, R. H., J. T. Gosling, E. Hildner, R. M. MacQueen, A. I. Poland, and C. L. Ross, The association of coronal mass ejection transients with other forms of solar activity, *Sol. Phys*., *61*, 201–215, 1979.

Paswaters, S. E., O. C. St. Cyr, R. A. Howard, G. E. Brueckner, and D. Wang, Analysis of halo coronal mass ejections observed by SOHO-LASCO, *Eos Trans. AGU*, *79*(17), Spring Meet. Suppl., S257, 1998.

Plunkett, S. P., et al., The relationship of green-line transients to white-light coronal mass ejections, *Sol. Phys*., *175*, 699–718, 1997.

Plunkett, S. P., B. J. Thompson, R. A. Howard, D. J. Michels, O. C. St. Cyr, S. J. Tappin, R. Schwenn, and P. L. Lamy, LASCO observations of an Earth-directed coronal mass ejection on May 12, 1997, *Geophys. Res. Lett*., *25*, 2477–2480, 1998.

Richardson, I. G., and H. V. Cane, Signatures of shock drivers in the

solar wind and their dependence on the solar source location, *J. Geophys. Res*., *98*, 15,295–15,304, 1993.
Russell, C. T. (Ed.), *The Global Geospace Mission*, vol. 71, Kluwer Acad., Norwell, Mass., 1995.
Schwenn, R., Mass ejections from the sun and their interplanetary counterparts, in *Solar Wind Eight*, edited by D. Winterhalter et al., *AIP Conf. Proc*., *382*, pp. 426–429, 1995.
Schwenn, R., et al., First view of the extended green-line emission corona at solar minimum using the LASCO-C1 coronagraph on SOHO, *Sol. Phys*., *175*, 667–684, 1997.
Sheeley, N. R., Jr., et al., Measurements of flow speeds in the corona between 2 and 30 Rs, *Astrophys. J*., *484*, 472–478, 1997.
Sheeley, N. R., Jr., J. H. Walters, Y.-M. Wang, and R. A. Howard, The continuous tracking of coronal outflows: Two kinds of coronal mass ejections, *J. Geophys. Res*., *104*, 24,739–24,767, 1999.
Sheeley, N. R., Jr., W. N. Hakala, and Y.-M. Wang, Detection of coronal mass ejection associated shock waves in the outer corona, *J. Geophys. Res*., *105*, 5081–5092, 2000.
Sime, D. G., and A. J. Hundhausen, The coronal mass ejection of July 6, 1980: A candidate for interpretation as a coronal shock wave, *J. Geophys. Res*., *92*, 1049–1055, 1987.
Simnett, G. M., et al., Disconnected magnetic structures out to beyond 28 solar radii during coronal mass ejections, *Sol. Phys*., *175*, 685–698, 1997.
Srivastava, N., R. Schwenn, B. Inhester, G. Stenborg, and B. Podlipnik, Measurements of flow speeds and acceleration in gradually evolving solar mass ejections as observed by LASCO, in *Solar Wind Nine*, edited by S. Habbal et al., *AIP Conf. Proc*., *471*, 115–118, 1999.
St. Cyr, O. C., and R. A. Howard, SOHO LASCO measurements of CME expansion, *Eos Trans. AGU*, *80*(46), Fall Meet. Suppl., F816, 1999.
St. Cyr, O. C., and A. J. Hundhausen, On the interpretation of "halo" coronal mass ejections, in *Solar Wind Six*, *Tech. Note NCAR/TN-306+Proc*, Natl. Cent. for Atmos. Res., Boulder, Colo., 1988.
St. Cyr, O. C., and D. F. Webb, Activity associated with coronal mass ejections at solar minimum: SMM observations from 1984–1986, *Sol. Phys*., *136*, 379–394, 1991.
St. Cyr, O. C., et al., White-light coronal mass ejections: A new perspective from LASCO, in *Eur. Space Agency Spec. Publ*., *ESA SP-415*, 103–110, 1997.
St. Cyr, O. C., J. T. Burkepile, A. J. Hundhausen, and A. R. Lecinski, A comparison of ground-based and spacecraft observations of coronal mass ejections from 1980–1989, *J. Geophys. Res*., *104*, 12,492–12,506, 1999.
Subramanian, P., K. P. Dere, N. B. Rich, and R. A. Howard, The relationship of coronal mass ejections to streamers, *J. Geophys. Res*., *104*, 22,321–22,330, 1999.
Tappin, S. J., and G. M. Simnett, The acceleration of CMEs in the outer corona as revealed by LASCO, *Eur. Space Agency Spec. Publ*., *ESA SP-415*, 117–120, 1997.
Thompson, B. J., S. P. Plunkett, J. B. Gurman, J. S. Newmark, O. C. St. Cyr, and D. J. Michels, SOHO/EIT observations of an Earth-directed coronal mass ejection on May 12, 1997, *Geophys. Res. Lett*., *25*, 2465–2468, 1998.
Thompson, B. J., J. B. Gurman, W. M. Neupert, J. S. Newmark, J.-P. Delaboudiniere, O. C. St. Cyr, S. Stezelberger, K. P. Dere, R. A. Howard, and D. J. Michels, SOHO/EIT observations of the 1997 April 7 coronal transient: Possible evidence of coronal Moreton waves, *Astrophys. J*., *517*, L151–L154, 1999a.
Thompson, B. J., O. C. St. Cyr, S. P. Plunkett, J. B. Gurman, N. Gopalswamy, H. S. Hudson, R. A. Howard, D. J. Michels, and J.-P. Delaboudiniere, The correspondence of EUV and white light observations of coronal mass ejections with SOHO EIT and LASCO, in *Sun-Earth Plasma Connections*, *Geophys. Monogr. Ser*., vol. 109, edited by J. L. Burch, R. L. Carovillano, and S. K. Antiochos, pp. 31–46, AGU, Washington, D. C., 1999b.
Wang, Y.-M., N. R. Sheeley, D. G. Socker, R. A. Howard, G. E. Brueckner, D. J. Michels, D. Moses, O. C. St. Cyr, A. Llebaria, and J.-P. Delaboudiniere, Observations of correlated white-light and extreme-ultraviolet jets from polar coronal holes, *Astrophys. J*., *508*, 899–907, 1998.
Wang, Y.-M., N. R. Sheeley Jr., R. A. Howard, N. B. Rich, and P. Lamy, Streamer disconnection events observed with the LASCO coronagraph, *Geophys. Res. Lett*., *26*, 1349–1352, 1999.
Webb, D. F., and E. W. Cliver, Evidence for magnetic disconnection of mass ejections in the corona, *J. Geophys. Res*., *100*, 5853–5870, 1995.
Webb, D. F., and R. A. Howard, The solar cycle variation of coronal mass ejections and the solar wind flux, *J. Geophys. Res*., *99*, 4201–4220, 1994.
Webb, D. F., E. W. Cliver, N. Gopalswamy, H. S. Hudson, and O. C. St. Cyr, The solar origin of the January 1997 coronal mass ejection, magnetic cloud and geomagnetic storm, *Geophys. Res. Lett*., *25*, 2469–2473, 1998.
Webb, D. F., E. W. Cliver, N. U. Crooker, O. C. St. Cyr, and B. J. Thompson, The relationship of halo CMEs, magnetic clouds, and magnetic storms, *J. Geophys. Res., 105*, 7491–7508, 2000.
Wood, B. E., M. Karovska, J. Chen, G. E. Brueckner, J. W. Cook, and R. A. Howard, Comparison of two coronal mass ejections observed by EIT and LASCO with a model of an erupting magnetic flux rope, *Astrophys. J*., *512*, 484–495, 1999.
Wu, S. T., et al., MHD interpretation of LASCO observations of a coronal mass ejection as a disconnected magnetic structure, *Sol. Phys*., *175*, 719–735, 1997.

J. B. Gurman and B. J. Thompson, Code 682, NASA Goddard, Greenbelt, Maryland 20771.
E. Hildner, NOAA Space Environment Center, 325 Broadway, Boulder, CO 80303.
R. A. Howard and N. R. Sheeley Jr., Naval Research Laboratory, 4555 Overlook Avenue, S.W., Washington, D.C. 20375.
M. J. Koomen, Sachs Freeman Associates, Naval Research Laboratory, 4555 Overlook Avenue, S.W., Washington, D.C. 20375.
P. L. Lamy, Laboratoire d'Astronomie Spatiale, Cedex 4, F-13248, Marseille, France.
D. J. Michels and S. P. Plunkett, Universities Space Research Association, Code 682.3, NASA Goddard, Greenbelt, Maryland 20771.
S. E. Paswaters, Ball Aerospace and Technologies Corporation, 1600 Commerce Street, Boulder, CO 80301.
R. Schwenn, Max Planck Institut fur Aeronomie, Postfach 20, Katlenburg-Lindau, Germany D-37189.
G. M. Simnett, School of Physics and Space Research, University of Birmingham, Birmingham, U. K. B15 2TT.
O. C. St. Cyr, Computational Physics, Inc., Code 682, NASA Goddard, Greenbelt, Maryland 20771.
D. F. Webb, AFRL/VSBS, 29 Randolph Road, Hanscom AFB, MA 01731.

(Received October 13, 1999; revised December 13, 1999;
accepted January 30, 2000.)